3D Printing in Medicine

RESEARCH

Open Access

3D printing of the brachial plexus and its osseous landmarks using magnetic resonance neurography for thoracic outlet syndrome evaluation

Nicole Wake[1,2*†], Yenpo Lin[3,4†], Ek T. Tan[3], Darryl B. Sneag[3], Sarah Ianucci[5] and Maggie Fung[1]

Abstract

Background Patient-specific three-dimensional (3D) printed anatomic models are valuable clinical tools that facilitate enhanced visualization of pertinent anatomic structures and have demonstrated benefits of reduced surgical times, increased surgeon confidence, and improved operative results and subsequent patient outcomes. Medical image-based 3D printed anatomic models are generally created from computed tomography (CT), however magnetic resonance imaging (MRI), which offers exquisite soft tissue characterization and flexible contrast avoiding the use of ionizing radiation, is an attractive alternative. Herein, the application of 3D printing incorporating both MR neurography and zero-echo time (ZTE) MRI for visualization of the brachial plexus anatomy in a subject with thoracic outlet syndrome (TOS) is described.

Methods A 28-year-old man presented with chronic right upper limb discomfort and paresthesias extending from the shoulder region to the third and fourth digits. The subject underwent evaluation with a unilateral brachial plexus MR neurography protocol at 3.0 Tesla for suspicion of TOS. The protocol included T2-weighted, 3D fast spin echo short-tau inversion recovery (STIR-FSE) and 3D radial ZTE sequences for depiction of the nerves and bones, respectively. The first rib and its synostosis impinged upon the inferior aspect of the T1 nerve root (T1NR), with accompanying mild enlargement of the T1NR. A 3D printed anatomic model was created and included: (1) bone (spine, ribs, clavicle, scapula, and humerus), (2) brachial plexus, and (3) costal cartilage.

Results The 3D printed model clearly demonstrated a T1NR impingement from the synostosis, confirming the diagnosis of neurologic thoracic outlet syndrome (TOS) and guided the treatment approach in prescribing TOS-specific physical therapy, which led to significant improvements in the patient's condition.

†Nicole Wake and Yenpo Lin contributed equally to this work and are designated as co-first authors.

*Correspondence:
Nicole Wake
Nicole.wake@gehealthcare.com

Full list of author information is available at the end of the article

Conclusion To our knowledge, this is the first in-vivo human 3D printed case for TOS using MRI-only data. The 3D printed model allowed for improved visualization and understanding of the spatial relationships between the nerves of the brachial plexus and surrounding osseous structures responsible for the patient's symptoms.

Clinical trial number Not applicable.

Keywords 3D printing, ZTE MRI, MR Neurography, Brachial plexus, Thoracic outlet syndrome

Introduction

Patient-specific three-dimensional (3D) printed anatomic models are valuable clinical tools that facilitate enhanced visualization of pertinent anatomic structures, thereby aiding surgeons in pre-operative planning and surgical simulation [1–3], enabling plate bending and device contouring for bone surgeries [4–6], assisting in device choice pre-operatively [7], and providing intraoperative reference [8]. 3D printed anatomic models have demonstrated benefits of reduced surgical times [9], increased surgeon confidence [3], and improved operative results and subsequent patient outcomes [9]. 3D printed anatomic models can also be used to improve patient communication [10] and facilitate medical education [11]. In orthopedic surgery, 3D printing has also been used for patient-matched implants [12, 13], total joint arthroplasty templating [14], and corrective osteotomy and fixation templating [15].

Medical image-based 3D printed anatomic models are generally created from computed tomography (CT). Anatomical regions of interest are segmented using the Hounsfield Unit scale and converted to file formats appropriate for 3D printing (e.g. STL, OBJ, VRML, etc.). Magnetic resonance imaging (MRI) is an attractive alternative, since it offers exquisite soft tissue characterization and flexible contrast avoiding the use of ionizing radiation [16, 17]. Additionally, there are several clinical scenarios for which MRI is used. For example, MRI may serve as the primary data for cardiac, neurological, and prostate 3D printing [16, 17]. In many other cases, even though the primary data is CT, MRI is used as an adjunct. For example, for patients with a superior sulcus (Pancoast) tumor, the location of the nerves in the brachial plexus is critical, as are the vessels and bony anatomy.

Segmentation from MRI techniques can be challenging due to the inherent low signal to noise ratio and noise in the raw images as well as the high similarities of image intensities among adjacent pertinent anatomical structures [16, 17]. Consequently, manual segmentation, a tedious and time-consuming task, must often be performed.

MR neurography techniques [18, 19] are being employed more frequently for the evaluation of neurologic disorders and nerve injury, including localizing pathologic nerve segments [20]. MR neurography uses high-resolution, T2-weighted, fat suppression and vascular suppression MRI techniques to visualize nerves throughout the body. Challenges in identifying the nerves, particularly those in the brachial plexus, can be met with dedicated MR neurography; and for the brachial plexus, MR neurography can significantly impact diagnostic and therapeutic management [21, 16, 17]. In particular, three-dimensional 3D MR neurography techniques [18, 19] can provide excellent nerve visualization, which with cinematic rendering, has been attempted to provide realistic visualization of peripheral nerves alongside nearby soft tissue structures [22]. Additionally, zero-echo time (ZTE) MRI [23] can be used to visualize bony structures accurately, due to its superior sensitivity to differentiate between osseous structures and other short-T2 soft tissue structures, compared to most other MRI sequences. Hence, rendering MR neurography together with ZTE-MRI can more accurately provide visualization of nerves alongside osseous anatomical landmarks [24].

In this work, we describe the application of 3D printing incorporating both MR neurography and ZTE MRI for visualization of the brachial plexus anatomy in a subject with neurogenic thoracic outlet syndrome (TOS) [25]. TOS refers to compression of the brachial plexus and/or accompanying vasculature [26], sometimes due to osseous anomalies, that lead to vascular and neurologic symptoms that may necessitate surgical intervention. As this syndrome involves the anatomic relationship between nerves and adjacent bones, 3D printing of both structures would provide the spatial context for the diagnosis and subsequent treatment and intervention.

Methods

A 28-year-old man presented with chronic right upper limb discomfort and paresthesias extending from the shoulder region to the third and fourth digits. After the patient underwent cervical spine MRI and electrodiagnostic findings that were normal, the patient underwent a unilateral brachial plexus MR neurography protocol at 3.0 Tesla (Signa Premier XT, GE HealthCare, Waukesha, WI, USA) to confirm the clinical suspicion of thoracic outlet syndrome.

The protocol included T2-weighted, 3D fast spin echo short-tau inversion recovery (STIR-FSE), and 3D radial zero-echo time (ZTE) sequences, both acquired at 1-mm-isotropic spatial resolution, for depiction of the nerves and bones, respectively. The patient was prospectively

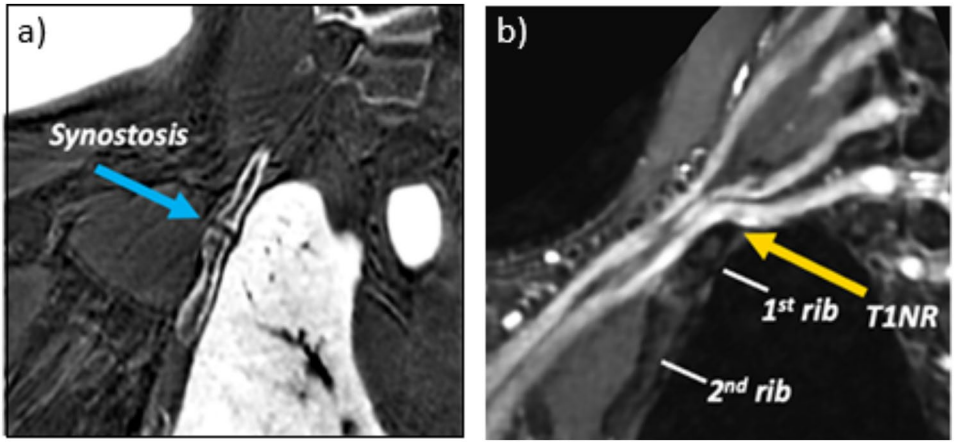

Fig. 1 (**a**) Coronal ZTE image demonstrating a first-second rib synostosis, (**b**) Coronal MR neurography image demonstrating impingement of the T1 nerve root (T1NR), as it combines with the C8 nerve root, to form the lower trunk by the first rib and its synostosis

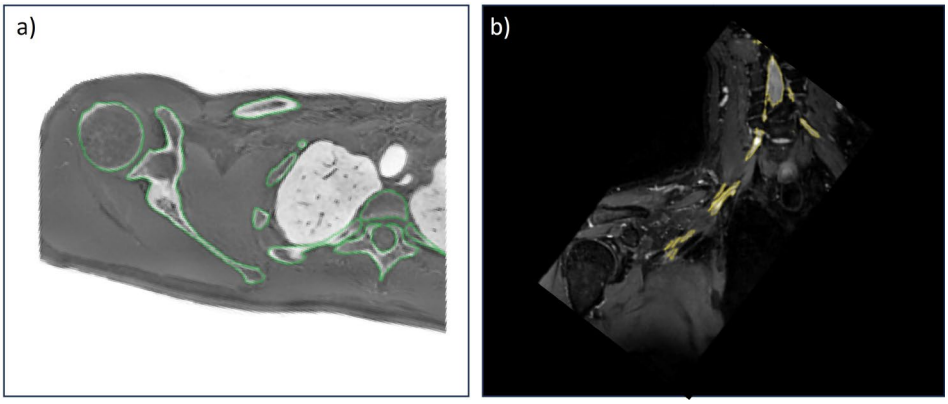

Fig. 2 (**a**) A representative ZTE MRI axial slice shows the outlined bone segmentation (green) and (**b**) a representative MR neurography coronal slice demonstrates the highlighted nerve segmentation (yellow)

recruited under an IRB-approved protocol, with written informed consent. Deep learning reconstruction (AIR Recon DL™, GE HealthCare, Waukesha, WI, USA) was applied in both 3D sequences, to reduce noise and enhance sharpness for optimal segmentation and 3D visualization [19].

The ZTE contrast was inverted during default image reconstruction to produce 'CT-like' images, showing a non-osseous synostosis between the right first and second ribs (Fig. 1a). The first rib and its synostosis impinged upon the inferior aspect of the T1 nerve root (T1NR), with accompanying mild enlargement of the T1NR (Fig. 1b). As the patient was considered for surgery, 3D rendering, segmentation, and multi-color 3D printing of MR neurography and ZTE were also performed.

In this case, the initial segmentation of the ZTE and the MR neurography images was performed on the GE Advantage Workstation (GE HealthCare, Waukesha, WI, USA) by an experienced radiologist (YL) and took approximately 50 min total, with 35 min spent on bone segmentation and 15 min on nerves. In addition, a cloud-based artificial intelligence (AI) based segmentation platform (Axial Insight, Axial3D, Belfast, Ireland) was utilized to generate the essential 3D data required for creating the 3D printed model, using the radiologist's segmentation for comparison. The DICOM MR images were securely uploaded to Axial3D's cloud-based INSIGHT platform, where they underwent automated quality assurance, PHI scrubbing, and initial review. The bony structures were segmented from ZTE and the nerves were segmented from MR neurography (Fig. 2); and a certified biomedical engineer (SI) independently validated the anatomical segmentation, using the initial segmentation performed by the radiologist as a guide.

Next, segmentations from MR neurography were overlaid on those from ZTE. Automatic image registration was performed via optimization of quality function of the matching between the two image sets (Amira, Thermo Fisher Scientific, Waltham, MA, USA). Image registration and segmentations were checked for accuracy to ensure anatomical landmarks in both datasets correctly aligned. Segmentations from both scans were converted

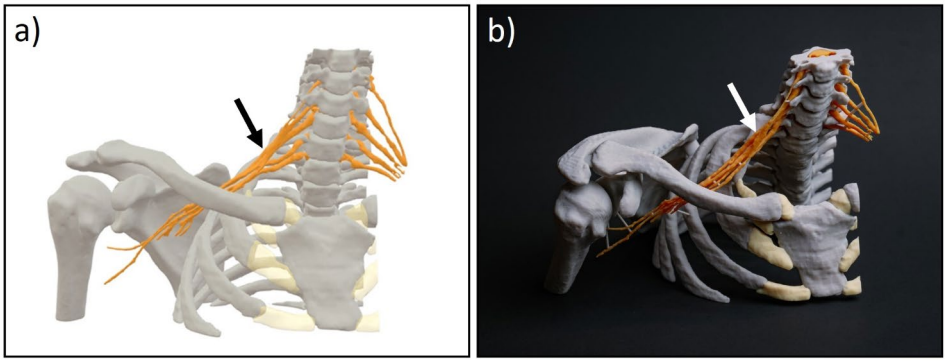

Fig. 3 (**a**) 3D representation of the anatomic model (Reproduced with permission from John Wiley and Sons, ref 25); (**b**) Photograph of the physical 3D printed model, with arrows indicating the area of impingement from the first-second rib synostosis

from binary masks to meshes and were combined into a single 3D model. For the anatomic model, three regions of interest were included: (1) bone (spine, ribs, clavicle, scapula, and humerus), (2) brachial plexus, and (3) costal cartilage. An initial 3D rendering of the model was verified by a biomedical engineer (SI) and shared with the radiologist (DBS) to ensure that all pertinent anatomic structures were adequately included with accuracy. The surgical team had access to review the 3D visualization directly through the INSIGHT platform, ensuring a seamless and efficient workflow. Multi-color 3D printing of the model was performed (J850, Stratasys, Rehovot, Israel).

Results

The final 3D printed model clearly demonstrated the T1NR impingement from the synostosis, confirming the diagnosis of neurologic TOS (Fig. 3). The model offered a more immersive and interactive way to visualize the brachial plexus and allowed for improved depth perception, enabling a better understanding of the spatial relationships between different anatomical structures.

While surgery was initially considered, it was not pursued as the primary treatment option by the referring surgeon. Instead, a specific TOS physical therapy regimen was initiated. After 2–3 weeks of therapy, the patient reported significant symptomatic improvement. After six months of therapy, the patient continued to improve and transitioned to a home exercise program.

Conclusion

To our knowledge, this is the first in-vivo human 3D printed case for TOS using MRI-only data. In this case, the patient initially received physical therapy for a shoulder labral tear, which did not improve symptoms. While the 3D printed model was not utilized for surgery, it demonstrated the spatial relationships between the nerves of the brachial plexus and surrounding osseous structures responsible for the patient's symptoms. The 3D printed model also demonstrated the potential for guiding the treatment approach in prescribing TOS-specific physical therapy, which led to significant improvements in the patient's condition. Besides guiding physical therapy, the 3D printed model can be used for patient education, which allows the physician/physical therapist to communicate the areas of nerve impingement that can help guide the patient about specific movements or positions to avoid, particularly during their home exercise program. This personalized approach, informed by the 3D model, may also enhance the effectiveness of a TOS-directed physical therapy.

This case highlighted the potential uses of advanced 3D modeling in personalized medicine for diagnostic evaluation, for patient and provider education, and for therapy and treatment planning. In the future, a quantitative clinical outcomes or follow-up study to assess the long-term impact of using 3D models in managing TOS would substantiate the clinical benefits discussed.

Acknowledgements
The authors thank Yan Wen, PhD, and Sagar Mandava, PhD for technical support.

Author contributions
NW wrote the main manuscript text. YL, ETT, DBS, MF, and NW edited the manuscript text. YL, ETT, and DBS were responsible for the data acquisition and interpretation. MF was responsible for protocol development, implementation, and interpretation of data. SI performed the image registration, segmentation, 3D modeling, and 3D printing. SI and DBS reviewed the segmentation and modeling for accuracy. MF, NW, YL, ETT, and DBS prepared the figures. All authors reviewed the manuscript and have approved the submitted version.

Funding
This study was conducted under an institutional research agreement between HSS and GE HealthCare.

Data availability
No datasets were generated or analysed during the current study.

Declarations

Ethics approval and consent to participate
The study was approved by Institutional Review Board of the Hospital for Special Surgery and individual consent for this study was obtained including consent for publication.

Competing interests
HSS has an institutional research agreement with GE HealthCare (YL, DBS, and ETT). Nicole Wake and Maggie Fung are Employees of GE HealthCare. Sarah Ianucci is an Employee of Axial3D. Darryl B. Sneag is a consultant for GE HealthCare.

Author details
[1]GE HealthCare, New York, NY, USA
[2]Center for Advanced Imaging Innovation and Research, New York University Langone Health, New York, NY, USA
[3]Department of Radiology and Imaging, Hospital for Special Surgery, New York, NY, USA
[4]Department of Medical Imaging and Intervention, Chang Gung Memorial Hospital, Taoyuan, Taiwan
[5]Axial3D, Belfast, UK

Received: 14 June 2024 / Accepted: 10 October 2024
Published online: 14 November 2024

References

1. Wake N, Rosenkrantz AB, Sodickson DK, Chandarana H, Wysock JS. MRI guided procedure planning and 3D simulation for partial gland cryoablation of the prostate: a pilot study. 3D Print Med. 2020;6:33.
2. Yoo SJ, Spray T, Austin EH 3rd, Yun TJ, van Arsdell GS. Hands-on surgical training of congenital heart surgery using 3-dimensional print models. J Thorac Cardiovasc Surg. 2017;153:1530–40.
3. Wake N, et al. 3D printed renal cancer models derived from MRI data: application in pre-surgical planning. Abdom Radiol (NY). 2017;42:1501–9.
4. Kraeima J, Glas HH, Witjes MJH, Schepman KP. Patient-specific pre-contouring of osteosynthesis plates for mandibular reconstruction: using a three-dimensional key printed solution. J Craniomaxillofac Surg. 2018;46:1037–40.
5. Numajiri T, et al. Using an In-House Approach to computer-assisted design and computer-aided Manufacturing Reconstruction of the Maxilla. J Oral Maxillofac Surg. 2018;76:1361–9.
6. Mackey C, et al. A Case Report describing pre-operative contouring of an Orthopedic Implant using a 3D-Printed patient-specific model. J Orthop Case Rep. 2021;11:27–31.
7. Mendonca CJA, et al. An overview of 3D anatomical Model Printing in Orthopedic Trauma surgery. J Multidiscip Healthc. 2023;16:875–87.
8. Leary OP, et al. Three-dimensional printed anatomic modeling for Surgical Planning and Real-Time Operative Guidance in Complex primary spinal column tumors: single-center experience and Case Series. World Neurosurg. 2021;145:e116–26.
9. Wake N, et al. Impact of 3D printed models on quantitative surgical outcomes for patients undergoing robotic-assisted radical prostatectomy: a cohort study. Abdom Radiol (NY). 2023;48:1401–8.
10. Wake N, et al. Patient-specific 3D printed and augmented reality kidney and prostate cancer models: impact on patient education. 3D Print Med. 2019;5:4.
11. Salazar D, Thompson M, Rosen A, Zuniga J. Using 3D Printing to improve Student Education of Complex anatomy: a systematic review and Meta-analysis. Med Sci Educ. 2022;32:1209–18.
12. Hamid KS, Parekh SG, Adams SB. Salvage of severe foot and ankle trauma with a 3D printed Scaffold. Foot Ankle Int. 2016;37:433–9.
13. Taunton MJ, et al. Pelvic discontinuity treated with custom triflange component: a reliable option. Clin Orthop Relat Res. 2012;470:428–34.
14. Narra SP, Mittwede PN, DeVincent Wolf S, Urish KL. Additive Manufacturing in Total Joint Arthroplasty. Orthop Clin North Am. 2019;50:13–20.
15. Li J, et al. 3D-printed model and osteotomy template technique compared with conventional closing-wedge osteotomy in Cubitus varus deformity. Sci Rep. 2022;12:6762.
16. Ripley B, et al. 3D printing from MRI Data: harnessing strengths and minimizing weaknesses. J Magn Reson Imaging. 2017;45:635–45.
17. Talanki VR, et al. Three-dimensional printed anatomic models derived from magnetic resonance Imaging Data: current state and Image Acquisition recommendations for Appropriate clinical scenarios. J Magn Reson Imaging. 2022;55:1060–81.
18. Filler AG, Maravilla KR, Tsuruda JS. MR neurography and muscle MR imaging for image diagnosis of disorders affecting the peripheral nerves and musculature. Neurol Clin. 2004;22:643–82. vi-vii.
19. Sneag DB et al. Optimized 3D brachial plexus MR neurography using deep learning reconstruction. Skeletal Radiol (2023).
20. Chhabra A, et al. Impact of high resolution 3 tesla MR Neurography (MRN) on diagnostic thinking and therapeutic patient management. Eur Radiol. 2016;26:1235–44.
21. Fisher S, Wadhwa V, Manthuruthil C, Cheng J, Chhabra A. Clinical impact of magnetic resonance neurography in patients with brachial plexus neuropathies. Br J Radiol. 2016;89:20160503.
22. Fritz J, Ahlawat S. High-resolution three-dimensional and cinematic rendering MR Neurography. Radiology. 2018;288:25.
23. Weiger M, Brunner DO, Dietrich BE, Muller CF, Pruessmann KP. ZTE imaging in humans. Magn Reson Med. 2013;70:328–32.
24. Lin Y, Sneag DB. Thoracic outlet Syndrome Associated with a Rib synostosis. Radiology. 2023;307:e223250.
25. Davidson EJ, Tan ET, Sneag DB. Magnetic resonance neurography in the diagnosis of neurological subtypes of thoracic outlet syndrome. Muscle Nerve (2024).
26. Ferrante MA, Ferrante ND. The thoracic outlet syndromes: part 1. Overview of the thoracic outlet syndromes and review of true neurogenic thoracic outlet syndrome. Muscle Nerve. 2017;55:782–93.

Publisher's note